Supramolecular Chemistry
Publication details, including instructions for authors and subscription information:
http://www.informaworld.com/smpp/title~content=t713649759

Conformational Preferences of Bispicolyl-*p*-*tert*-butylcalix[4]arene Anions: Synthesis of Cone and Partial-cone Conformers of Bispicolyl-bis-(*tert*-butoxycarbonyl)methoxy-*p*-*tert*-butylcalix[4]arene

Juan Olguín[a]; Hugo Vázquez Lima[b]; Alonso Rubio[a]; Simón Hernández-Ortega[a]; Patricia Guadarrama[b]; Ivan Castillo[a]
[a] Instituto de Química, Universidad Nacional Autónoma de México, Circuito Exterior, Ciudad Universitaria, México D. F., México [b] Instituto de Investigaciones en Materiales, Universidad Nacional Autónoma de México, Circuito Exterior, Ciudad Universitaria, México D. F., México

To cite this Article Olguín, Juan , Lima, Hugo Vázquez , Rubio, Alonso , Hernández-Ortega, Simón , Guadarrama, Patricia and Castillo, Ivan(2007) 'Conformational Preferences of Bispicolyl-*p*-*tert*-butylcalix[4]arene Anions: Synthesis of Cone and Partial-cone Conformers of Bispicolyl-bis-(*tert*-butoxycarbonyl)methoxy-*p*-*tert*-butylcalix[4]arene', Supramolecular Chemistry, 19: 8, 587 — 597

To link to this Article: DOI: 10.1080/10610270601169683

URL: http://dx.doi.org/10.1080/10610270601169683

Supramolecular Chemistry, December 2007 Vol. 19 (8), pp. 587–597

Taylor & Francis
Taylor & Francis Group

Conformational Preferences of Bispicolyl-*p*-*tert*-butylcalix[4]arene Anions: Synthesis of Cone and Partial-cone Conformers of Bispicolyl-bis-(*tert*-butoxycarbonyl)methoxy-*p*-*tert*-butylcalix[4]arene

JUAN OLGUÍN[a], HUGO VÁZQUEZ LIMA[b], ALONSO RUBIO[a], SIMÓN HERNÁNDEZ-ORTEGA[a],
PATRICIA GUADARRAMA[b,*] and IVAN CASTILLO[a,*]

[a]*Instituto de Química, Universidad Nacional Autónoma de México, Circuito Exterior, Ciudad Universitaria, México D. F. 04510, México;* [b]*Instituto de Investigaciones en Materiales, Universidad Nacional Autónoma de México, Circuito Exterior, Ciudad Universitaria, México D. F. 04510, México*

(Received 11 October 2006; Accepted 13 December 2006)

The disubstituted calix[4]arene derivative 5,11,17,23-tetra-*tert*-butyl-25,27-dihydroxy-26,28-bis(2-pyridyl methoxy)calix[4]arene 2, which crystallises in the monoclinic space group $P2_1/n$, was functionalised in the phenolic O—H groups with (*tert*-butoxycarbonyl)-methoxy groups. The yield of the isolated cone and partial-cone conformers of tetrasubstituted 5,11,17,23-tetra-*tert*-butyl-25,27-bis[(*tert*-butoxycarbonyl)methoxy]-26,28-bis(2-pyridylmethoxy)calix[4]arene 3a and 3b, depends on the identity of the alkali metal hydride employed to deprotonate 2. Partial-cone conformer 3b crystallises in the monoclinic space group $P2_1/n$, with an inverted (*tert*-butoxycarbonyl)methoxy-containing phenol moiety. The product distribution of 3a and 3b was interpreted based on the relative stabilities of the alkali metal complexes with the doubly deprotonated derivative of 2, and the monoanionic derivative [(*tert*-butoxycarbonyl)methoxy-2]$^-$, by molecular mechanics analysis.

Keywords: Calixarenes; Calixanions; Conformers; Crystal structure; Molecular mechanics

INTRODUCTION

Calixarenes and their derivatives are an important class of compounds due to their versatility as ligands in main group and transition metal chemistry [1–3], and as building blocks in supramolecular chemistry [4,5], among other fields. In addition, the pre-organised structure of the calixarenes has led to the development of molecular receptors with convergent recognition sites [4]. In this context, the regioselective substitution of the phenolic positions of *p*-*tert*-butylcalix[4]arene **1** has allowed the introduction of a variety of functional groups, which include ethers, ketones, esters, carboxylic acids, amines, amides, and several nitrogen-containing heterocycles [6–8].

The regioselective introduction of substituents in alternate phenolic positions of **1** is a well established transformation. In the specific case of the bispicolyl derivative **2**, the synthetic procedure reported results in the formation of the cone conformer (Scheme 1). Since the steric bulk of the picolyl groups locks them on the same side of the macrocycle, further functionalisation could potentially lead to the formation of cone or partial-cone tetrasubstituted conformers. Deprotonation of the remaining hydroxy groups with alkali metal compounds typically represents the first step in the complete substitution of disubstituted calix[4]arene derivatives. Thus, the nature of the interaction between calixarene-derived anions and alkali metals must play an important role in determining the regio- and stereoselectivity of the products. Unfortunately, the interaction of guests with calixarene-derived anions has not been extensively studied [9–11], despite the numerous reports that address the thermodynamics of the interaction between neutral calixarenes and several guest molecules and ions [12].

---

*Corresponding authors. E-mail: joseivan@servidor.unam.mx; patriciagua@correo.unam.mx

ISSN 1061-0278 print/ISSN 1029-0478 online © 2007 Taylor & Francis
DOI: 10.1080/10610270601169683

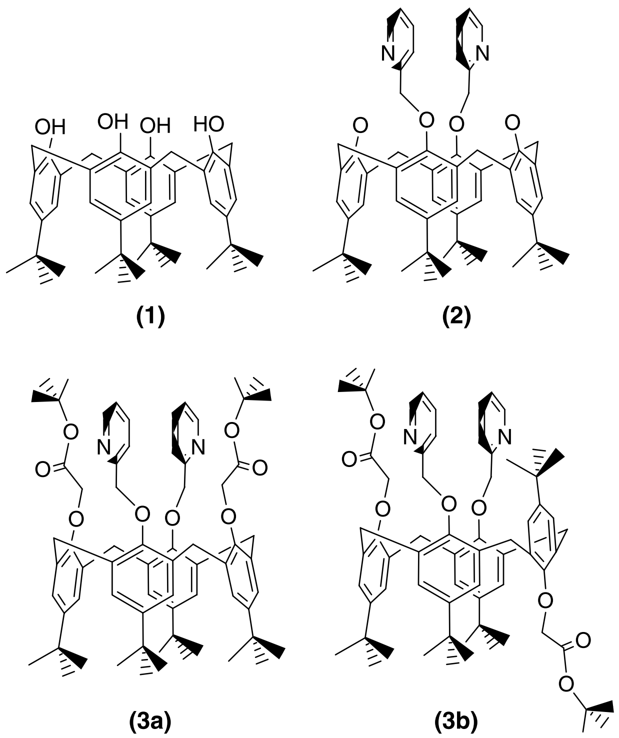

SCHEME 1 Schematic representation of compounds **1**–**3b**.

Herein we report the effect of different alkali metal hydrides on the deprotonation and functionalisation of the previously reported 5,11,17,23-tetra-*tert*-butyl-25,27-dihydroxy-26,28-bis(2-pyridylmethoxy)calix[4]arene **2** [13,14], which adopts a cone conformation in the solid state. Reaction of the phenoxide groups of deprotonated **2** with *tert*-butylbromoacetate results in both cone **3a**, and partial-cone **3b** conformers of the tetrasubstituted 5,11,17,23-tetra-*tert*-butyl-25,27-bis[(*tert*-butoxycarbonyl)methoxy]-26,28-bis(2-pyridylmethoxy)calix[4]arene in varying ratios.

RESULTS AND DISCUSSION

Synthesis of Tetrasubstituted 3a and 3b

The synthesis of the bispicolyl derivative **2** from the parent *p*-*tert*-butylcalix[4]arene **1** has been reported by several authors [13,14], but the conditions described in the experimental section avoid the use of the high-boiling solvent dimethylformamide (DMF), and allow the isolation of **2** in high yield. Its identity was established by melting point determination, NMR and IR spectroscopy.

In order to establish the effect of the alkali metal on the substitution of the available phenolic positions, both O—H groups of **2** were deprotonated with LiH, NaH, and KH. Analogous studies have been conducted previously with alkali metal carbonates, i.e. Li_2CO_3, Na_2CO_3, K_2CO_3, and Cs_2CO_3, with DMF and acetone as solvents [13–15]. When LiH was used as the base, reaction of deprotonated **2** with *tert*-butylbromoacetate led predominantly to the formation of compound **3a** (24%). In all synthetic procedures of **3a** and **3b**, unreacted **2** was obtained from the reaction mixture. In the case of **3a**, the yield is further affected by the isolation of variable amounts of a solid tentatively formulated as **3a**·LiBr (*vide infra*). The cone conformation of this product was determined by ^{1}H NMR spectroscopy [13]: the relatively simple spectrum of **3a** corresponds to an idealised C_2 symmetry, with two doublets corresponding to the bridging methylene protons at δ 3.99 ppm and 3.08 ppm, respectively. The ^{13}C NMR spectrum confirms the cone conformation of **3a** based on the 23 resonances observed, which are consistent with a pseudo-C_2 symmetry in solution. Exclusive formation of the cone conformer **3a** with the small Li^+ cation is consistent with previous observations [13], which attribute the stereoselectivity to a template effect. In our system compound **3a** appears to form a complex **3a**·LiBr, which was obtained as pink microcrystals. Although NMR spectra of this complex in $CDCl_3$ are characterised by broad resonances from 213 to 338 K, analysis by FAB mass spectrometry allowed us to detect a molecular ion at m/z 1066, which corresponds to [**3a**·LiBr]$^+$. Further characterisation of this compound will be reported elsewhere.

In previous studies employment of sodium bases resulted in the stereoselective preparation of tri- and tetrasubstituted derivatives of **2** in cone conformation [14]. In contrast, the deprotonation of **2** with NaH, followed by treatment with *tert*-butylbromoacetate, resulted in the formation of both cone **3a**, and partial-cone **3b** conformers in approximately equal amounts. The isolated yields were 23% and 25%, respectively, after separation by column chromatography on silica gel eluted with a gradient of hexanes/ethyl acetate (9:1–1:1 v/v). As in the case of **3a**, the structure of **3b** was initially determined by ^{1}H NMR spectroscopy. The presence of four sets of doublets, which correspond to the bridging methylene protons, is indicative of the partial cone conformation in solution [13]. The diastereotopic $—OCH_2—$ protons of the picolyl groups give rise to two doublets with geminal coupling ($J = 11.6$ Hz) centered at δ 4.79 and 4.89 ppm, while the $—OCH_2—$ protons of the ester groups give rise to two singlets at δ 4.27 and 4.36 ppm. In the ^{13}C NMR spectrum, the presence of 17 aromatic, 15 aliphatic, and 2 carbonyl signals is consistent with the proposed partial-cone structure. Definitive confirmation of the structure of **3b** was obtained in the solid state by X-ray crystallography.

The analogous reaction of **2** with KH as the base results in the exclusive formation of the partial-cone conformer **3b** after treatment with *tert*-butylbromoacetate in 45% yield, possibly by a template effect. The partial-cone conformation of **3b** requires a

TABLE I Crystal data and structure refinement for compounds **2** and **3b**

	2	**3b**
Formula	$C_{58}H_{69}N_3O_4$	$C_{68}H_{86}N_2O_8$
Molecular weight	872.16	1059.39
Crystal system	Monoclinic	Triclinic
Space group	$P2_1/n$	$P\text{-}1$
Wavelength (Å)	0.71073	0.71073
Crystal colour	Colourless	Colurless
T (K)	291(2)	291(2)
Crystal dimensions (mm)	0.35 × 0.26 × 0.11	0.40 × 0.38 × 0.32
a (Å)	13.6706(7)	14.2191(8)
b (Å)	16.4243(8)	14.4870(8)
c (Å)	22.9039(12)	17.5203(10)
α (°)	90	80.178(1)
β (°)	96.928(1)	80.002(1)
γ (°)	90	63.134(1)
V (Å^3)	5105.1(4)	3153.1(3)
hkl ranges	$-16 \leq h \leq 16$ $-19 \leq k \leq 9$ $-27 \leq l \leq 27$	$-16 \leq h \leq 16$ $-17 \leq k \leq 7$ $-20 \leq l \leq 20$
ρ_{calc} (g cm^{-3})	1.135	1.116
Z	4	2
F(000)	1880	1144
μ (mm^{-1})	0.070	0.072
θ range (°)	1.53 to 25.00	1.58 to 25.00
Independent reflections	8991	11090
Data/restraints/ parameters	8991/198/652	11090/810/929
Goodness-of-fit on F^2	0.801	0.957
R	0.0428	0.0808
R_w	0.0746	0.1738
Largest diff. peak and hole (e Å^{-3})	0.139 and −0.146	0.262 and −0.150

TABLE II Selected bond lengths (Å) and angles (°) for compounds **2** and **3b**

Compound **2**			
O1—C1	1.375(2)	C12—O2—C45	112.4(1)
O2—C12	1.398(2)	C34—O4—C52	112.4(2)
O2—C45	1.435(2)	N47—C46—C51	123.3(2)
O3—C23	1.371(2)	N47—C46—C45	115.0(2)
O4—C34	1.402(2)	N54—C53—C58	123.3(2)
O4—C52	1.438(2)	N54—C53—C52	113.1(2)
N47—C46	1.322(2)	O2—C45—C46	110.2(2)
N47—C48	1.331(3)	O4—C52—C53	111.4(2)
N54—C53	1.319(3)		
N54—C55	1.344(3)		
Compound **3b**			
O1—C45	1.432(4)	C1—O1—C45	111.6(2)
O2—C65	1.394(4)	C34—O2—C65	113.7(3)
O3—C58	1.406(5)	C23—O3—C58	111.2(3)
O4—C52	1.397(4)	C12—O4—C52	118.9(3)
O5—C53	1.200(5)	O5—C53—O6	123.0(5)
O6—C53	1.307(5)	O5—C53—C52	125.4(5)
O6—C54	1.458(5)	O7—C66—O8	121.8(9)
O7—C66	1.250(11)	O7—C66—C65	115.3(8)
O8—C66	1.278(9)	O2—C65—C66	112.1(5)
O8—C67	1.495(6)	O4—C52—C53	118.6(4)
N47—C46	1.388(7)	N47—C46—C45	107.5(5)
N47—C48	1.431(9)	N47—C46—C51	104.7(6)
N60—C59	1.366(6)	N60—C59—C58	115.4(6)
N60—C61	1.372(7)	N60—C59—C64	121.9(5)

longer distance between the oxygen atom in the inverted phenol moiety and the rest of the oxygen atoms in the calixarene framework. This results in a larger cavity, which presumably accommodates the large K$^+$ cation, and determines the stereoselectivity observed.

Solid State Structures of 2 and 3b

Although the solid state structures of **2** co-crystallised with 1,4-dibromo and 1,4-diiodotetrafluorobenzene have been reported [16], the structure of the disubstituted macrocycle on its own remains unknown. We obtained X-ray quality crystals of **2** from acetonitrile; selected crystallographic data are presented in Table I. The presence of the cone conformer in the solid state is in agreement with the structure in solution, as determined by ^{1}H NMR spectroscopy. This conformation is stabilised by the presence of two intramolecular hydrogen bonds between the phenol O—H groups as donors, and the ethereal oxygen atoms as acceptors. The nitrogen atoms of the picolyl groups are directed away from the macrocyclic cavity, as a face to face orientation would result in significant repulsion between the corresponding lone pairs. A list of selected bond distances and angles is presented in Table II, and the molecular structure of compound **2** with atom numbering scheme is presented in Fig. 1. As is commonly observed in *p-tert*-butylcalix[n]arenes, two of the *tert*-butyl groups of **2** have rotational disorder and were modeled in two positions.

Crystals of **3b** were obtained by slow evaporation of a 1:1 hexane/ethyl acetate solution. The partial-cone conformation determined by spectroscopic methods is confirmed in the solid state, with one of the (*tert*-butoxycarbonyl)methoxy-containing phenol moieties inverted with respect to the calix[4]arene

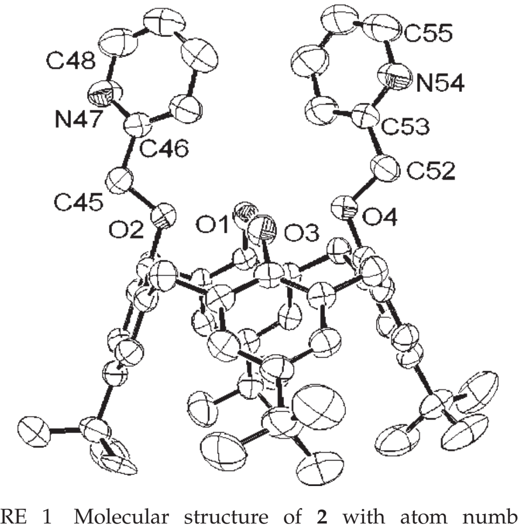

FIGURE 1 Molecular structure of **2** with atom numbering scheme, minor-occupancy disordered atoms, hydrogen atoms, and a molecule of acetonitrile are omitted for clarity. Thermal ellipsoids are drawn at the 50% probability level.

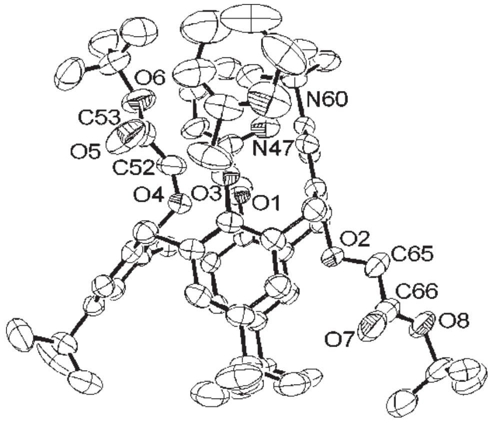

FIGURE 2 ORTEP diagram of **3b** at the 50% probability level, with minor-occupancy disordered carbon, nitrogen, and oxygen atoms, as well as hydrogen atoms omitted for clarity.

framework. O8 and C66 of this group were modeled in two positions, while the carbonyl O atom was modeled in three positions. The pyridyl group defined by N47—C51 was modeled in two, and all but one of the *tert*-butyl groups (C20—C22) presented rotational disorder. An ORTEP diagram of **3b** with atom numbering scheme is presented in Fig. 2. Additional crystallographic data are presented in Table I, and a selected list of bond lengths and angles is presented in Table II.

Computational Studies

In order to determine the effect of the alkali metal cation on the observed ratios of the cone and partial-cone conformers of **3**, an initial theoretical approximation was carried out involving the exploration of the potential energy surface, considering two cases: (i) conversion of the fully-deprotonated dianionic form of **2** in cone conformation (two metal alkoxides with M = Li$^+$, Na$^+$, and K$^+$) to the hypothetic partial-cone conformer of the dianion, as illustrated in Figs 3 and S1; and (ii) conversion of the monosubstituted, monoanionic derivative [(*tert*-butoxycarbonyl)methoxy-**2**]$^-$ (one metal alkoxide, M = Li$^+$, Na$^+$, and K$^+$) from cone to partial-cone conformation, Figs. 3 and S2.

After initial energy minimisation by Molecular Mechanics (force field MMFFs) [17], the conformational conversion from cone to partial-cone was achieved by the simultaneous rotation of the two dihedral angles marked in grey in Fig. S5, varied in incremental steps of 5 degrees. The total energy as a function of the dihedral angle was plotted for each metal cation, considering the two scenarios (i) and (ii) mentioned before. For each case, two minima corresponding to cone and partial-cone conformations are observed, as well as a maximum related to the barrier of interconversion between the two structures. Although these maxima do not correspond formally to the transition states, they set a limit for the highest potential energy allowed for the actual transition states.

To ensure that the structures located at the valleys of the plots correspond to energetic minima, a MonteCarlo [18] conformational search was carried out with the algorithm of multiple minima (MCMM) [19,20], using the same force field (MMFFs). Since none of the force fields in molecular mechanics take into account the electronic energy, only the comparison of relative energies results in a meaningful conformational analysis. The ΔE values (calculated as $E_{cone} - E_{partial\text{-}cone}$, $E_{cone} - E_{barrier}$, and $E_{partial\text{-}cone} - E_{barrier}$) for the different conformers are shown in Tables III and IV. For the transformation of the

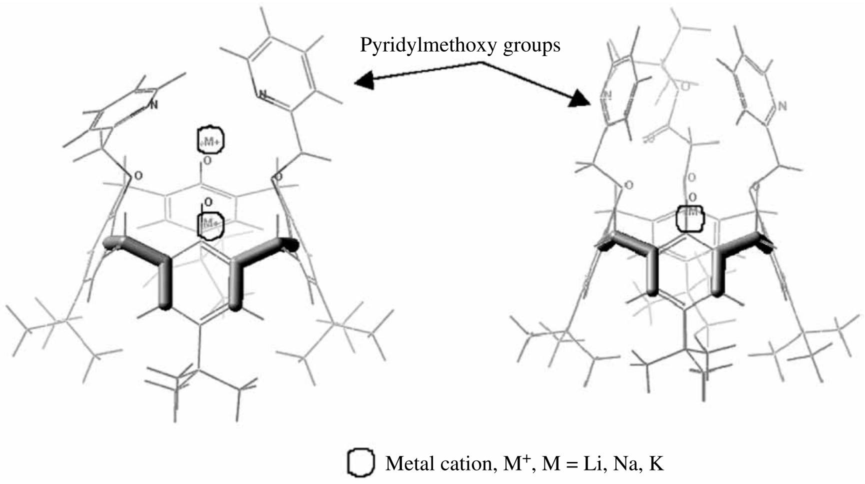

(a) (b)

FIGURE 3 Dihedral angles (marked grey) varied to determine the energetic profile for: (a) dianionic derivative of **2**, and (b) monoanionic [(*tert*-butoxycarbonyl)methoxy-**2**]$^-$.

TABLE III Energetic parameters for the doubly deprotonated derivative of **2** (kJ/mol)

Metal cation	$\Delta E_{\text{cone/partial-cone}}$	$\Delta E_{\text{cone/barrier}}$	$\Delta E_{\text{partial-cone/barrier}}$
Li^+	34.798	53.590	18.790
Na^+	17.994	68.011	50.017
K^+	10.322	84.030	73.712

cone conformer of dianionic **2** into the partial-cone conformer in scenario (i), the energetic profiles calculated are very similar for all counter-cations. In terms of ΔE, the calculated stability of the dianionic cone conformer diminishes relative to that of the partial-cone one as the metal cation changes from Li^+ to K^+, with ΔE varying from 34.80 to 10.32 kJ/mol (Table III and Fig. S3).

The potential energy surface corresponding to scenario (ii), when one (*tert*-butoxycarbonyl)-methoxy substituent is already present, is shown in Fig. S4. As calculated for (i), the stability of the cone conformer diminishes on going from Li^+ to K^+ (Table IV). In the particular case of K^+ there is an inversion of the energy of the two minima, with the partial-cone conformer being more stable by 10.86 kJ/mol. This outcome is probably due to the combination of a large cation and the steric hindrance introduced by the (*tert*-butoxycarbonyl)methoxy substituent on the calix[4]arene framework. In addition, cation–π interactions can play an important role in the conformational preferences of calixarenes [21].

According to the experimental observations, the yield of cone conformer (compound **3a**) decreases as the metal cation changes from Li^+, Na^+ to K^+(24%, 23%, and 0%, respectively). It is evident from the data in Table III that although the cone conformer is more stable in the series of dianionic derivatives of **2**, regardless of the countercation, the difference in energy between the two minima decreases. Thus, the partial-cone conformation becomes progressively favoured as the size of the metal cation increases. When the mono-substituted, mono-anionic series is considered (Table IV), the same trend is observed. In this latter case the effect is more pronounced, since an inversion in energetic position of the minima is predicted by the calculations. This would lead to predominant formation of the partial-cone conformer, consistent with the isolation of **3b** when KH was used as the base.

TABLE IV Energetic parameters for the monosubstituted derivative [(*tert*-butoxycarbonyl)methoxy-**2**]$^-$ (kJ/mol)

Metal cation	$\Delta E_{\text{cone/partial-cone}}$	$\Delta E_{\text{cone/barrier}}$	$\Delta E_{\text{partial-cone/barrier}}$
Li^+	29.220	95.210	65.989
Na^+	16.000	108.228	92.228
K^+	−10.857	97.147	108.004

CONCLUSIONS

The incorporation of (*tert*-butoxycarbonyl)methoxy groups to the phenolic positions of disubstituted calix[4]arene **2** can be performed stereoselectively based on the choice of alkali metal hydride. Cone and partial-cone conformers of the tetrasubstituted calixarene, **3a** and **3b**, can be obtained by employing either LiH or KH to deprotonate the phenolic O—H groups. The solid state structure of **2** reveals the presence of intramolecular O—H···O hydrogen bonds, which stabilise it in a cone conformation. In the case of **3b**, its solid state structure confirms the assignment in solution as a partial-cone conformer.

Potential energy profiles calculated for the dianionic derivative of **2**, and the monoanionic derivative [(*tert*-butoxycarbonyl)methoxy-**2**]$^-$, are mainly influenced by two factors: the steric bulk of the (*tert*-butoxycarbonyl)methoxy group, and the nature of the cation coordinated to the anionic macrocycles. Of these two factors, the latter appears to direct the stereoselectivity, which leads to the cone and partial-cone conformers **3a** and **3b**. It is important to note that the effect of the alkali metal arises from the cation size, as well as cation–π interactions with the aromatic groups of the calixarene [21]. Nonetheless, a molecular mechanics approach can help predicting the preferred conformations for substituted calix[4]arenes.

EXPERIMENTAL

General

p-tert-Butylcalix[4]arene **1**, 2-(chloromethyl)pyridine hydrochloride, *tert*-butylbromoacetate, potassium iodide, potassium carbonate, as well as lithium, sodium, and potassium hydrides were purchased from Aldrich Chemical Co., and were used without further purification. Acetone was dried over 4 Å molecular sieves, tetrahydrofuran (THF) was dried over sodium/benzophenone ketyl, and both solvents were distilled under an atmosphere of dinitrogen prior to use.

Melting points were determined on an Electrothermal Mel-Temp apparatus and are uncorrected. ^1H and ^{13}C NMR spectra were recorded on a JEOL Eclipse 300 spectrometer in $CDCl_3$ with tetramethylsilane as an internal standard. Infrared spectra (KBr disks) were recorded on a Perkin–Elmer 203-B spectrometer in the 4000–400 cm^{-1} region, and positive ion fast atom bombardment (FAB) mass spectra were obtained on a JEOL JMS-SX-102A mass spectrometer operated at an accelerating voltage of 10 kV. Samples were desolved from a nitrobenzyl alcohol matrix by using xenon atoms at 6 keV.

*Synthesis of 5,11,17,23-tetra-*tert*-butyl-25,27-dihydroxy-26,28-bis(2-pyridylmethoxy)calix[4]arene 2*

To a suspension of **1** (1.00 g, 1.44 mmol) in 25 mL of dry acetone was added an excess of K_2CO_3 (1.50 g, 14.00 mmol) under an N_2 atmosphere, and the reaction mixture was stirred for an hour. Solid 2-(chloromethyl)pyridine hydrochloride (0.52 g, 3.17 mmol) was added, as well as a catalytic amount of KI, and the mixture was refluxed for 20 h. Upon cooling to room temperature, the pink solution was filtered through a pad of celite, and the volatile materials were removed under reduced pressure. The white solid obtained was washed with 2 × 20 mL of methanol, and recrystallised from hot hexanes.

Yield: 0.92 g (77%); mp = 253–254°C (lit. 250–252°C [13]).

*General Description of the Synthesis of Cone and Partial Cone 5,11,17,23-tetra-*tert*-butyl-25,27-bis[(*tert*-butoxycarbonyl)methoxy]-26,28-bis(2-pyridylmethoxy)calix[4]arene 3a and 3b*

To a suspension of compound **2** (210 mg, 0.25 mmol) in 25 mL of dry THF were added 2 equivalents of LiH (**3a**) or KH (**3b**) (0.50 mmol) under an N_2 atmosphere, and the mixture was stirred at room temperature until evolution of H_2 subsided. *tert*-Butylbromoacetate (0.65 mL, 0.50 mmol) was added *via* syringe, and the reaction mixture was refluxed for 14 h. After cooling to room temperature, the mixture was filtered, and the volatile materials were evaporated under reduced pressure. Compound **3a** was obtained by washing the off-white solid obtained with 2 × 2 mL of hexanes, 3b was isolated by trituration of the reaction mixture with ca. 2 mL of methanol.

3a Yield: 65 mg (24%); mp 209–210°C; IR (KBr): 3052, 2960, 2907, 2869, 1731, 1594, 1479, 1440, 1395, 1366, 1303, 1260, 1195, 1157, 1127, 1059, 975, 948, 869, 834, 773, 751, 637, 609, 579, 517, 460; ^{1}H NMR (300 MHz, $CDCl_3$): 8.67 (2H, d, $J = 4.1$ Hz, Py—H), 7.70 (2H, m, Py—H), 7.33 (2H, m, Py—H), 7.00 (10H, m, Ar—H/Py—H), 5.13 (4H, s, O—CH_2), 4.34 (4H, s, O—CH_2), 3.99 (4H, d, $J = 12.4$ Hz, CH_2), 3.08 (4H, d, $J = 12.4$ Hz, CH_2), 1.64 (18H, s, O-*t*-Bu), 1.09 (18H, s, *t*-Bu), 1.05 (18H, s, *t*-Bu); ^{13}C{^{1}H} NMR (75 MHz, $CDCl_3$): 170.5, 155.8, 155.5, 150.8, 149.9, 148.8, 148.6, 148.1, 136.9, 134.6, 134.3, 125.9, 124.1, 123.7, 84.3, 79.1, 73.2, 34.2, 31.2, 29.9, 29.7, 28.4, 28.1. Anal. Calcd. for $C_{68}H_{86}N_2O_8$ (%): C, 77.09; H, 8.18; N, 2.64. Found: C, 77.03; H, 8.42; N, 2.52.

3b Yield: 120 mg (45%); mp 252–253°C; IR (KBr): 3050, 2957, 2906, 2869, 1756, 1593, 1477, 1366, 1309, 1287, 1260, 1195, 1154, 1067, 1014, 949, 871, 849, 799, 773, 749, 702, 639, 607, 555, 517, 403; ^{1}H NMR (300 MHz, $CDCl_3$): 8.64 (2H, m, Py—H), 7.69 (4H, m, Py—H), 7.13 (2H, d, $J = 2.8$ Hz, Py—H), 7.05 (2H, s, Ar—H), 7.00 (2H, s, Ar—H), 6.51 (2H, d $J = 2.4$ Hz, Ar—H), 4.89 (2H, d, $J = 11.6$ Hz, CH_2), 4.79 (2H, d, $J = 11.6$ Hz, CH_2), 4.43 (2H, d, $J = 13.0$ Hz, CH_2), 4.36 (4H, s, O—CH_2), 4.27 (4H, s, O—CH_2), 3.91 (2H, d, $J = 13.5$ Hz, CH_2), 3.71 (2H, d, $J = 13.5$ Hz, CH_2), 3.16 (2H, d, $J = 13.0$ Hz, CH_2), 1.45 (9H, s, *t*-Bu), 1.33 (9H, s, *t*-Bu), 1.16 (9H, s, *t*-Bu), 1.04 (18H, s, *t*-Bu), 0.93 (9H, s, *t*-Bu); ^{13}C{^{1}H} NMR (75 MHz, $CDCl_3$): 169.9, 168.7, 157.9, 155.3, 153.4, 152.0, 149.2, 144.6, 143.2, 136.7, 135.0, 132.6, 131.7, 131.6, 128.3, 126.2, 125.6, 123.3, 122.7, 81.2, 80.4, 77.4, 70.7, 68.5, 36.9, 34.1, 33.9, 33.7, 32.3, 31.8, 31.5, 31.3, 28.2, 28.0. Anal. Calcd. for $C_{68}H_{86}N_2O_8$ (%): C, 77.09; H, 8.18; N, 2.64. Found: C, 77.20; H, 7.88; N, 2.59.

X-ray Crystallography

Single crystals were mounted at room temperature on a Bruker SMART diffractometer equipped with an Apex CCD area detector. Frames were collected by omega scans, and integrated with the Bruker SAINT software package [22] using the appropriate unit cell. The structures were solved using the SHELXS-97 program [23], and refined by full-matrix least-squares on F^2 with SHELXL-97 [24]. Weighted *R*-factors, *R*w, and all goodness of fit indicators, *S*, were based on F^2. The observed criterion of ($F^2 > 2\sigma F^2$) was used only for calculating the *R*-factors. All non-hydrogen atoms were refined with anisotropic thermal parameters in the final cycles of refinement. Hydrogen atoms were placed in idealised positions, with C—H distances of 0.93 Å and 0.98 Å for sp^2 and sp^3 hybridised carbon atoms, respectively. The isotropic thermal parameters of the hydrogen atoms were assigned the values of $U_{\text{iso}} = 1.2$ times the thermal parameters of the parent non-hydrogen atom.

Computational Details

All initial structures were constructed and equilibrated by Molecular Mechanics (force field MMFFs) [17]. The used force field has two important features included in its parameterisation: (i) calculations with full geometry optimisation at high levels of theory (e.g. MP2/6-31G*) for equilibrium conformers, and (ii) non-covalent interactions calculations using highly correlated wave functions. In order to validate the use of MMFFs, the structure of **2** was theoretically minimised and superimposed to the X-ray structure obtained experimentally. A very good geometrical concordance was observed (Fig. S5).

The calculated RMS value (Root-Mean-Square, measure of the maximum difference between superimposed atom positions) corresponding to the superimposed structure minimised with MMFFs was 0.834323 when C, N and O atoms are considered. This small deviation is in accordance with that observed in Fig. S5. The other superimposed structures correspond to those optimised by DFT method (BHandHLYP/6-31G*, and BHandHLYP/6-31G** levels), whose RMS values are 1.053 and 0.664, respectively. Thus, geometry optimisation with both Molecular Mechanics and DFT methods provide comparable results.

With MMFFs as minimisation tool, the Macromodel software package was used to map out the potential energy surface varying the two dihedral angles marked in Fig. 3. This process involved stepping through the dihedral angles, and for each combination of values, the angles were constrained while a minimisation was performed.

SUPPLEMENTARY DATA

Calculated potential energy plots, schematic representations of calculated structures of anionic derivatives of **2**, and calculated structure of **2** superimposed to the X-ray crystallographic structure. Crystallographic data for compounds **2** and **3b** have been deposited with the Cambridge Crystallographic Data Centre, CCDC reference numbers 202414 and 202415. Copies of this information may be obtained free of charge from: The Director, CCDC, 12 Union Road, Cambridge, CB2 1EZ, UK (fax: +44-1233-336033; deposit@ccdc.cam.ac.uk or http://www.ccdc.cam.ac.uk).

Acknowledgements

The authors thank Luis Velasco and Javier Pérez for help with mass spectrometry measurements. JO, AR, and IC thank DGAPA-UNAM (IN247402) for financial support; JO thanks CONACyT (181982) for additional financial support.

References

[1] Wieser, C.; Dieleman, C. B.; Matt, D. *Coord. Chem. Rev.* **1997**, *165*, 93.

[2] Redshaw, C. *Coord. Chem. Rev.* **2003**, *244*, 45.

[3] Sliwa, W. *J. Incl. Phenom. Macr. Chem.* **2005**, *52*, 13.

[4] Hosseini, M. W. *Acc. Chem. Res.* **2005**, *38*, 313.

[5] Organo, V. G.; Leontiev, A. V.; Sgarlata, V.; Dias, H. V. R.; Rudkevich, D. M. *Angew. Chem. Int. Ed.* **2005**, *44*, 3043.

[6] Gutsche, C. D. *Calixarenes*; Royal Society of Chemistry: London, 1989.

[7] Gutsche, C. D. In *Calixarenes Revisited*; Stoddart, J. F., Ed.; Royal Society of Chemistry: Cambridge, 1998.

[8] Asfari, Z., Böhmer, V., Harrowfield, J., Vicens, J., Eds.; *Calixarenes 2001*; Kluwer: Dordrecht, 2001.

[9] Thuéry, P.; Asfari, Z.; Vicens, J.; Lamare, V.; Dozol, J. -F. *Polyhedron* **2002**, *21*, 2497.

[10] Gueneau, E. D.; Fromm, K. M.; Goesmann, H. *Chem. Eur. J.* **2003**, *9*, 509.

[11] Hanna, T. A.; Liu, L.; Angeles-Bonza, A. M.; Kou, X.; Gutsche, C. D.; Ejsmont, K.; Watson, W. H.; Zakharov, L. N.; Incarvito, C. D.; Rheingold, A. L. *J. Am. Chem. Soc.* **2003**, *125*, 6228.

[12] Danil de Namor, A. F.; Cleverley, R. M.; Zapata-Ormachea, M. L. *Chem. Rev.* **1998**, *98*, 2495.

[13] Shinkai, S.; Fujimoto, K.; Otsuka, T.; Ammon, H. L. *J. Org. Chem.* **1992**, *57*, 1516.

[14] Pappalardo, S.; Giunta, L.; Foti, M.; Ferguson, G.; Gallagher, J. F.; Kaitner, B. *J. Org. Chem.* **1992**, *57*, 2611.

[15] Fujimoto, K.; Nishiyama, N.; Tsuzuki, H.; Shinkai, S. *J. Chem. Soc. Perkin 2* **1992**, 643.

[16] Messina, M. T.; Metrangolo, P.; Pappalardo, S.; Parisi, M. F.; Pilati, T.; Resnati, G. *Chem. Eur. J.* **2000**, *6*, 3495.

[17] Halgren, T. A. *J. Comput. Chem.* **1996**, *17*, 490.

[18] Kolossváry, I.; Guida, W. C. *J. Am. Chem. Soc.* **1996**, *118*, 5011.

[19] Chang, G.; Guida, W. C.; Still, W. C. *J. Am. Chem. Soc.* **1989**, *111*, 4379.

[20] Saunders, M.; Houk, K. N.; Wu, Y. D.; Still, W. C.; Lipton, M.; Chang, G.; Guida, W. C. *J. Am. Chem. Soc.* **1990**, *112*, 1419.

[21] Macias, A. T.; Norton, J. E.; Evanseck, J. D. *J. Am. Chem. Soc.* **2003**, *125*, 2351.

[22] Bruker AXS. *SAINT Software Reference Manual v. 6.23C*; Madison, WI, 2002.

[23] Sheldrick, G. M. SHELXS-97. *Crystal Structure Solution, Version 97-1*; Institut Anorg. Chemie. University of Gottingen: Germany, 1990.

[24] Sheldrick, G. M. SHELXL-97. *Crystal Structure Refinement, Version 97-1*; Institut Anorg. Chemie. University of Gottingen: Germany, 1997.

APPENDIX

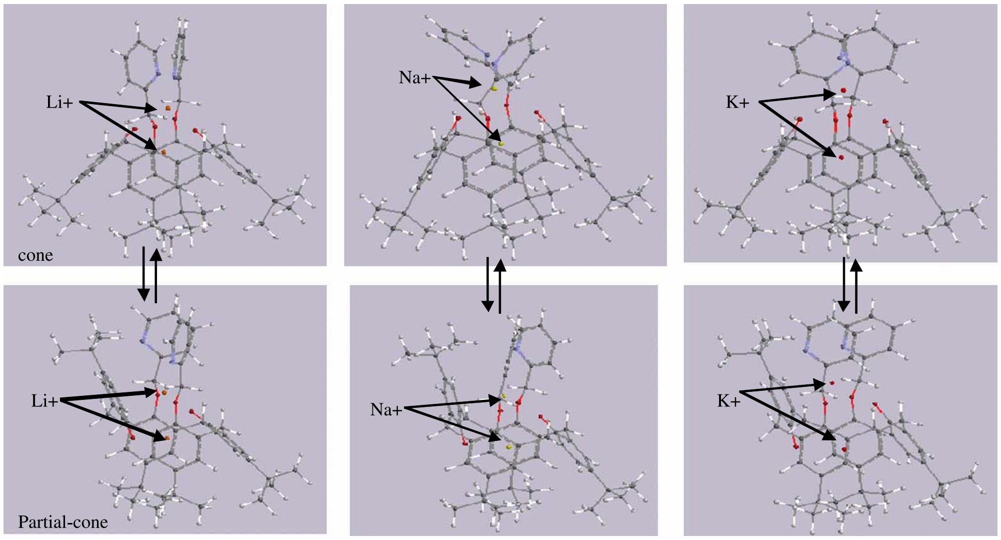

FIGURE S1 Schematic representation of the interconversion of cone to partial-cone conformers of the doubly deprotonated form of **2** with Li^+, Na^+, and K^+ as counterions.

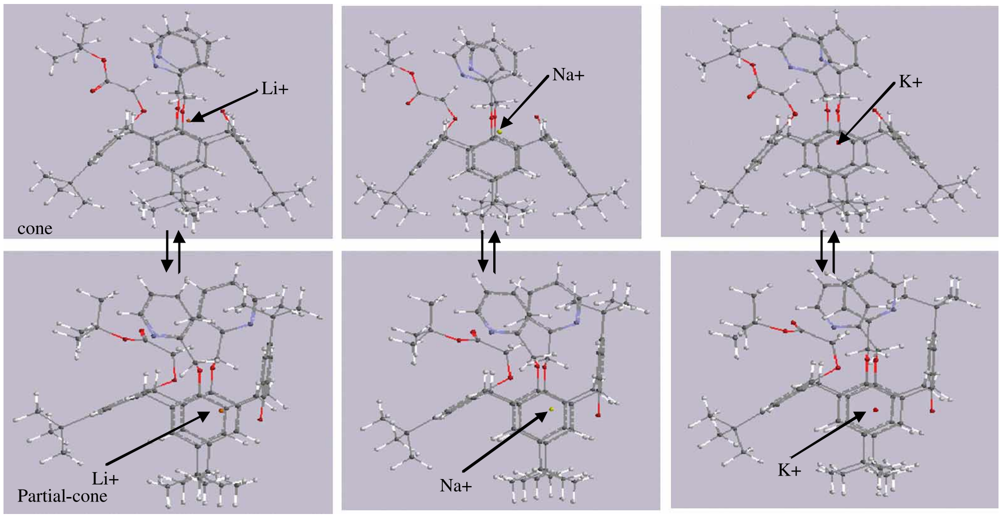

FIGURE S2 Schematic representation of the interconversion of cone to partial-cone conformers of the monoanionic species [(*tert*-butoxycarbonyl)methoxy-**2**]$^-$ with Li^+, Na^+, and K^+ as counterions.

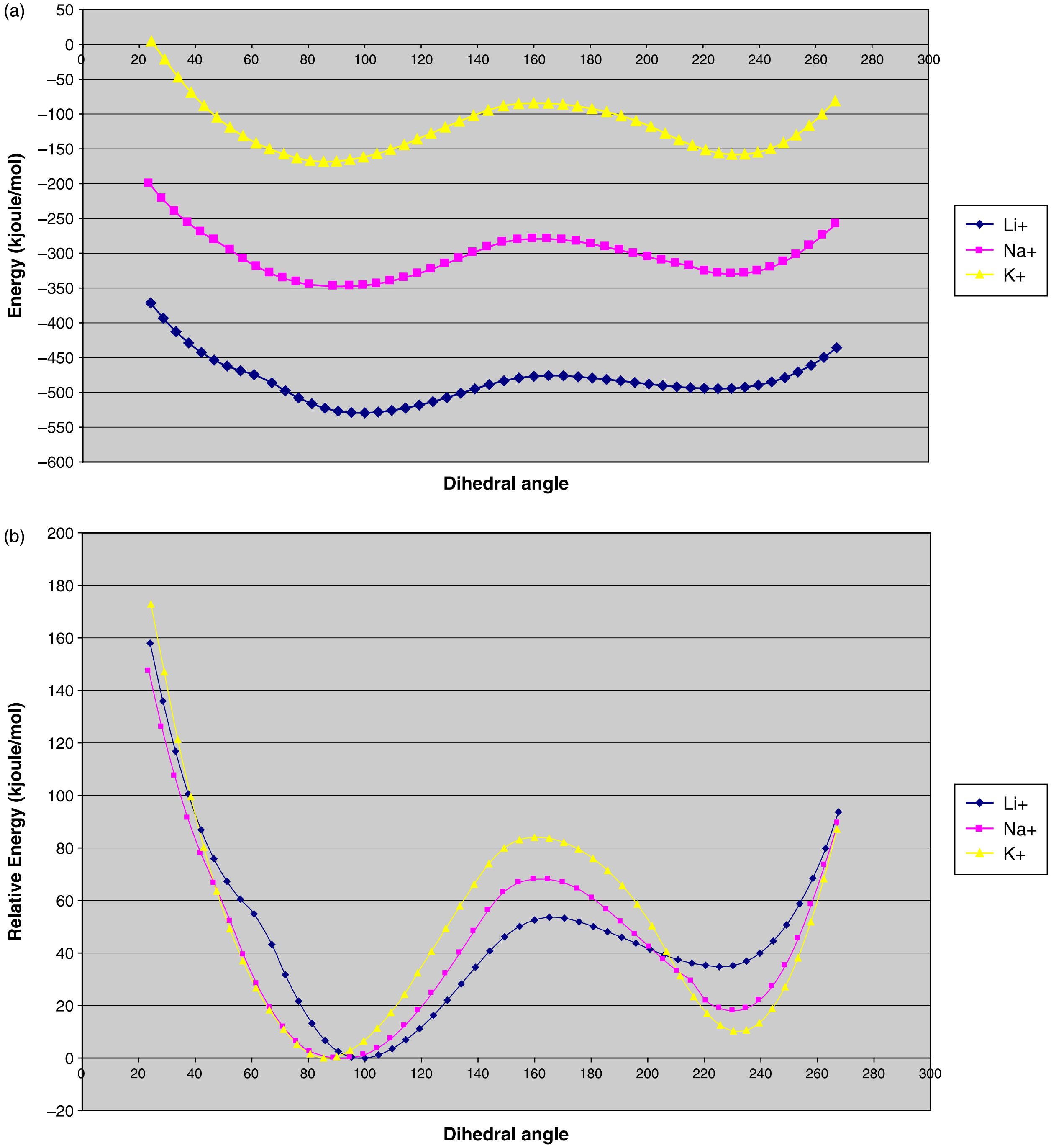

FIGURE S3 Plots of (a) potential energy of the cone and partial-cone conformers of the dianionic derivative of **2**, and (b) relative energies.

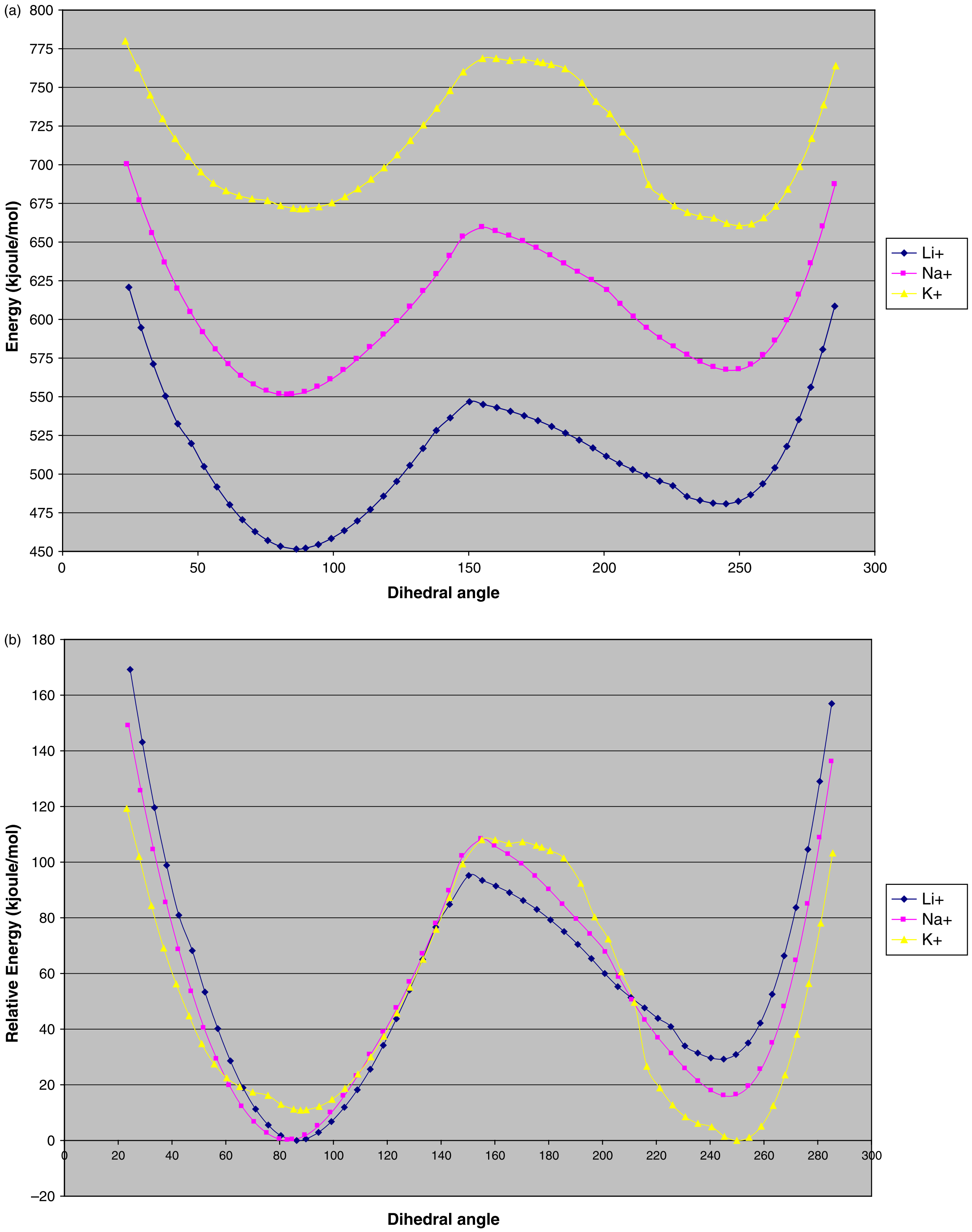

FIGURE S4 Plots of (a) potential energy of the cone and partial-cone conformers of the monoanionic derivative [(*tert*-butoxycarbonyl)methoxy-**2**]$^-$, and (b) relative energies.

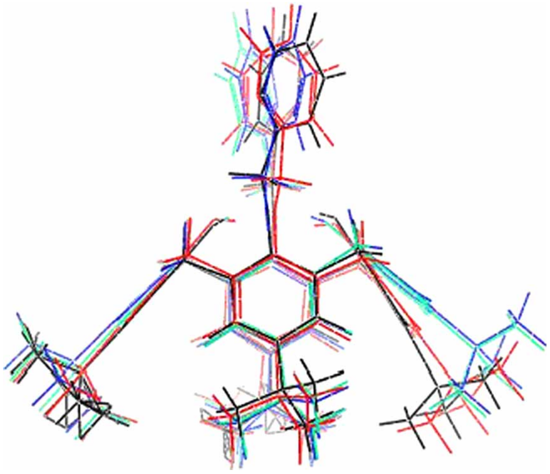

FIGURE S5 X-ray structure of compound **2** (black) and superimposed structures optimised at Molecular Mechanics (MMFFs) level (red), BHandHLYP/6-31G* level (blue), and BHandHLYP/6-31G** level (green).